

Nonclassical characteristic functions for highly sensitive measurements

Th. Richter and W. Vogel

*Arbeitsgruppe Quantenoptik, Fachbereich Physik,
Universität Rostock, D-18051 Rostock, Germany*

(Dated: January 29, 2007)

Abstract

Characteristic functions are shown to be useful for highly sensitive measurements. Redistributions of motional Fock states of a trapped atom can be directly monitored via the most fragile nonclassical part of the characteristic function. The method can also be used for decoherence measurements in optical quantum-information systems.

PACS numbers: 42.50.Dv, 03.67.-a, 42.50.Vk

The experimental demonstrations of photon antibunching [1], sub-Poissonian photon statistics [2] and quadrature squeezing [3] also led to an increasing interest in practical applications of nonclassical states. An early example is the proposal to use squeezed light for enhancing the sensitivity of interferometric gravitational-waves detection [4]. Experiments have demonstrated the usefulness of squeezed light for improving interferometric measurements [5, 6] and spectroscopy [7].

Two decades after the first experimental demonstrations of the potential usefulness of nonclassical states the latter still play a minor role in practical measurements. There may be several reasons for this fact. First, the experimental effort for generating the needed nonclassical states is rather high. Second, some applications, e.g. the use of squeezed light for optimizing the laser power in gravitational-wave detection, can be replaced with developments of laser sources. Third, nonclassical states are usually highly fragile against losses which may substantially limit their advantages in some applications.

The use of nonclassical states is frequently considered in the context of the reduction of the quantum noise in a certain observable below an ultimate classical noise limit. Examples are the use of sub-Poissonian and squeezed light fields for reducing the noise in direct and homodyne photodetection, respectively. This requires to link the measurement principle with the observable whose quantum noise is reduced. Below we will reconsider the application of nonclassical states from a much broader point of view. When speaking about nonclassical states in the following, we will only consider quantum states of a single-mode harmonic oscillator whose Glauber-Sudarshan P -function is not a probability density [8].

The nonclassicality of quantum states can be completely characterized in terms of measurable characteristic functions of the phase-dependent quadrature distributions. To be more specific, necessary and sufficient conditions have been derived that completely characterize the nonclassicality of a given quantum state in terms of the quadrature characteristic function $G(k, \varphi)$ [9]. A broad class of nonclassical states can be well characterized by the rather simple condition of first-order nonclas-

sicality: the absolute value of the characteristic function exceeds, for some arguments, the corresponding value of the ground (or vacuum) state [10],

$$|G(k, \varphi)| \geq G_{\text{gr}}(k). \quad (1)$$

The signatures of first-order nonclassicality are more general than the quantum-noise reduction of a chosen observable below some classical limit. The condition also includes features like quantum interference [11] and sub-Planck structures in phase space [12]. Note that the nonclassicality condition (1) has been applied in experiments [13].

In the following we will study highly sensitive measurement principles, which are using the fragility of nonclassical parts of characteristic functions as a sensitive probe. The method is analyzed for sensitive detections of both the vibrational-state redistributions of a trapped ion and the decoherence of nonclassical light during its propagation. Such possibilities are of interest for the diagnostics of decoherence in quantum information systems.

The direct measurement of the characteristic function of the quantized center-of-mass motion of a trapped ion has been proposed [14] and realized [15]. An electronic transition is simultaneously driven on the red and the blue motional sidebands in the resolved sideband regime, which is described by the interaction Hamiltonian

$$\hat{H}_{\text{int}} = \hbar \left(\Omega \hat{A}_{12} + \Omega^* \hat{A}_{21} \right) \hat{x}_\varphi, \quad (2)$$

where $\hat{A}_{ij} = |i\rangle\langle j|$ ($i, j = 1, 2$) is the electronic flip operator and Ω is the effective Rabi frequency. Most importantly, it is proportional to the phase-dependent quadrature operator of the center-of-mass motion,

$$\hat{x}_\varphi = \hat{a} e^{i\varphi} + \hat{a}^\dagger e^{-i\varphi}, \quad (3)$$

\hat{a} (\hat{a}^\dagger) is the annihilation (creation) operator for the ion's motion. The phase φ is controlled by the phase difference of the driving lasers.

Let us assume that the ion is initially prepared in the separable state $\hat{\rho}(0) = \hat{\rho}(0) \otimes \hat{\sigma}(0)$, with $\hat{\rho}(0)$ and $\hat{\sigma}(0)$ being the vibrational and electronic states respectively.

The observation of the time evolution of the occupation $\sigma_{11}(t, \varphi)$ of the electronic ground state $|1\rangle$ directly yields a measurement of the characteristic function $G(k, \varphi)$ of the quadrature distribution [14]:

$$G(k, \varphi) = 2 \left[\sigma_{11}^{(\text{inc})}(k, \varphi) - \frac{1}{2} \right] + 2i \left[\sigma_{11}^{(\text{coh})}(k, \varphi) - \frac{1}{2} \right], \quad (4)$$

the time being scaled as $k = 2|\Omega|t$. The incoherent and coherent occupations, $\sigma_{11}^{(\text{inc})}$ and $\sigma_{11}^{(\text{coh})}$, are measured with the initial electronic preparations $\sigma_{11}(0) = 1$ and $\sigma_{11}(0) = |\sigma_{12}(0)| = \frac{1}{2}$, respectively. The electronic-state occupations in Eq. (4) are obtained with almost perfect efficiency, by testing a transition from state $|1\rangle$ to an auxiliary state for the appearance of fluorescence [15].

Now we will consider this measurement procedure for the highly sensitive detection of the occupation redistribution of the motional quantum states. Note that the observed decoherence of a Raman-driven trapped ion [16] is not completely understood yet. Whereas dephasing mechanisms could be identified [17], deeper insight in the role of motional states is required.

To illustrate the basic idea, let us deal with a simple model of the vibrational-state redistribution, caused by a thermal bath of finite temperature and mean occupation number \bar{n} . The density operator $\hat{\rho}$ for the ion's center-of-mass motion in the interaction picture obeys the master equation

$$\begin{aligned} \frac{d}{dt} \hat{\rho} = & \gamma (\bar{n} + 1) [2\hat{a}\hat{\rho}\hat{a}^\dagger - \hat{a}^\dagger\hat{a}\hat{\rho} - \hat{\rho}\hat{a}^\dagger\hat{a}] \\ & + \gamma \bar{n} [2\hat{a}^\dagger\hat{\rho}\hat{a} - \hat{a}\hat{a}^\dagger\hat{\rho} - \hat{\rho}\hat{a}\hat{a}^\dagger], \end{aligned} \quad (5)$$

with γ being the damping rate. This model is useful since exact solutions are available for it. The measurement principle under study, however, may sensitively detect any other redistribution mechanism as well.

Transforming the master equation into an equation for the Wigner characteristic function, $\chi(\xi, t) \equiv \text{Tr} \{ \hat{\rho} \exp(\xi \hat{a}^\dagger - \xi^* \hat{a}) \}$, the solution is given by [18]

$$\begin{aligned} \chi(\xi, t) = & \exp \{ -(\bar{n} + 1/2) |\xi|^2 [1 - \exp(-2\gamma t)] \} \\ & \times \chi(\xi \exp(-\gamma t), 0), \end{aligned} \quad (6)$$

where $\chi(\xi, 0)$ is the Wigner characteristic function of the initial quantum state. The Wigner characteristic function $\chi(\xi)$ and the quadrature characteristic function $G(k, \varphi)$ are related to each other via [11]

$$G(k, \varphi) = \chi(ik e^{-i\varphi}). \quad (7)$$

In the following we are interested in a trapped atom which is initially in the number state $|m\rangle$, which has been realized in experiments [16]. The motional state redistributions caused by the reservoir lead to strong modifications of the nonclassical signatures of the characteristic function, being the highly sensitive probe in our method.

The Wigner characteristic function of the initial number state $|m\rangle$ is given by

$$\chi_m(\xi) = L_m(|\xi|^2) \exp(-|\xi|^2/2), \quad (8)$$

where $L_m(x)$ is a Laguerre polynomial of order m . Clearly, the quadrature characteristic function of the number state $|m\rangle$ is phase independent, $G_m(k, \varphi) = G_m(k)$. In Fig. 1 we show the quadrature characteristic functions $G_m(k)$ as a function of k for the number states with $m = 9, 10, 11$. In all cases $|G_m(k)|$ clearly exceeds, for some values of k , the classical bound according to Eq. (1). This represents the first-order nonclassicality of the number states. For the number state $|10\rangle$ the first-order nonclassical effect is most pronounced at $k \approx 6$, where the quadrature characteristic function $G_{10}(k)$ has a local maximum and the absolute deviation from the classical limit, $G_{\text{gr}}(k)$, attains its maximum. For the neighbouring number states, $|9\rangle$ and $|11\rangle$, the function $G_m(k)$ attains almost the same absolute values around $k \approx 6$, however, with opposite sign.

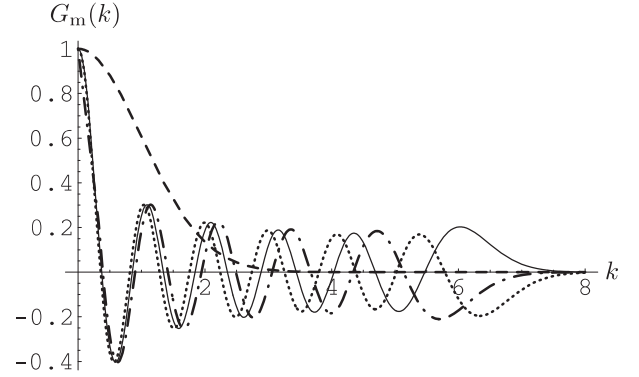


FIG. 1: Characteristic functions $G_m(k)$ versus k for number states $m = 10$ (full line), 9 (dashed-dotted) and 11 (dotted), together with the classical limit $G_{\text{gr}}(k) = e^{-k^2/2}$ (dashed).

Let us consider the time evolution of the characteristic function $G_m(k, t)$, where the subscript m indicates the initial number state $|m\rangle$, in contact with a thermal reservoir of mean occupation number \bar{n} . The initial preparation of a Fock state $|m\rangle$ allows one to distinguish motional-state redistribution effects from dephasing effects. Using Eqs. (6), (7) the time-dependent characteristic function $G_m(k, t)$ of an initial number state $|m\rangle$ coupled to a thermal reservoir is given by

$$\begin{aligned} G_m(k, t) = & \exp \{ -\bar{n} [1 - \exp(-2\gamma t)] k^2 \} \\ & \times L_m(k^2 e^{-2\gamma t}) \exp(-k^2/2). \end{aligned} \quad (9)$$

To get more insight into the time evolution, we consider the time derivative of the characteristic function at $t = 0$,

$$\dot{G}_m(k, 0) = 2\gamma [L_{m-1}^{(1)}(k^2) - \bar{n} L_m(k^2)] k^2 e^{-k^2/2}. \quad (10)$$

The initial time derivative strongly depends on both k and \bar{n} , for $m = 10$ its maximum occurs at $k_{\text{max}} \approx 6$.

Comparison with Fig. 1 shows that the characteristic function reacts most sensitively on a redistribution of the motional-state occupations in the outermost maximum of the initial characteristic function, where the nonclassical behavior is most pronounced. This is a reflection of the expected high fragility of nonclassical signatures of the quadrature characteristic function.

It may be interesting to compare the time evolution of the nonclassical characteristic function with the time evolution of the sub-Poissonian statistics. Its measurement might be expected to be the optimum for observing occupation redistributions among the number states. For the Mandel parameter, $Q = (\langle(\Delta\hat{n})^2\rangle - \langle\hat{n}\rangle)/\langle\hat{n}\rangle$, which measures the deviation from the Poissonian statistics, we get

$$Q(t) = \frac{(\bar{n}^2 - 2\bar{n}m - m)e^{-4\gamma t} + 2\bar{n}(m - \bar{n})e^{-2\gamma t} + \bar{n}^2}{me^{-2\gamma t} + \bar{n}(1 - e^{-2\gamma t})}. \quad (11)$$

Negative values of Q characterize a nonclassical quantum state with sub-Poissonian statistics.

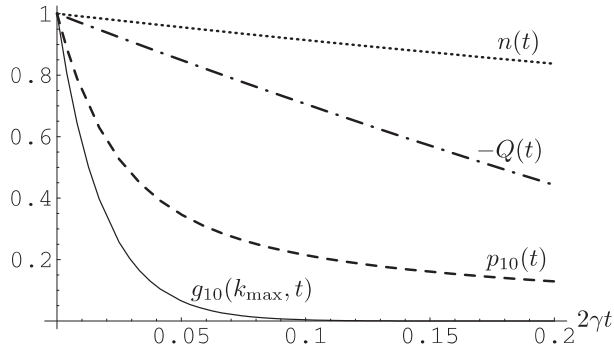


FIG. 2: Time evolution of the occupation probability $p_{10}(t)$ of the initially prepared number state $|m = 10\rangle$, the normalized mean excitation number $n(t)$, the Mandel parameter $Q(t)$, and the normalized characteristic function $g_{10}(k_{\max}, t)$, for $\bar{n} = 1$.

In Fig. 2 we show the time evolution of the normalized characteristic function, $g_{10}(k, t) = G_{10}(k, t)/G_{10}(k, 0)$, for $k = k_{\max}$ and $\bar{n} = 1$. For comparison, the time evolution of the Mandel Q parameter, of the occupation probability $p_{10}(t)$ of the initially prepared Fock state $|m = 10\rangle$, and the normalized mean motional-state excitation $n(t)$, $n(t) = \langle\hat{n}(t)\rangle/\langle\hat{n}(0)\rangle$ with $\langle\hat{n}(t)\rangle = me^{-2\gamma t} + \bar{n}(1 - e^{-2\gamma t})$, are shown for $\bar{n} = 1$ as well. It is clearly seen that the nonclassical characteristic function shows the fastest decay and evolves much faster than the nonclassical property described by the Mandel Q parameter. In fact, the nonclassical signatures of the quadrature characteristic function decay even faster than the occupation probability of the initially prepared Fock state, so that the measured characteristic function is more sensitive even as a number-state measurement that is matched to the initial nonclassical state. Note that for other k -values,

which are within the classical region (such as $k \approx 1$) or that violate the classical limit only slightly (e.g. $k \approx 2$), the temporal evolution of the characteristic function is significantly slower.

How can we explain the highly sensitive behavior of the characteristic function in its outermost maximum? The quadrature characteristic function under consideration can be written in the form

$$G_{10}(k, t) = \sum_{n=0}^{\infty} p_n(t) G_n(k), \quad (12)$$

as a sum of characteristic functions of the number states weighted with the occupation probabilities $p_n(t)$. The characteristic functions $G_9(k)$ and $G_{11}(k)$ for the Fock states neighboring the initial one appear to have the opposite sign at $k = k_{\max} \approx 6$ compared with $G_{10}(k)$, cf. Fig. 1. Hence the motional-state redistribution, leading to increasing values of $p_9(t)$ and $p_{11}(t)$, results in a faster decay of $G_{10}(k_{\max}, t)$ compared with the decay of $p_{10}(t)$.

So far we have considered the use of nonclassical characteristic functions for the highly sensitive detection of motional-state redistributions of trapped ions. In this case the preparation of Fock states is rather simple and the detection of the characteristic function is easily performed exactly in the needed, most sensitive point $k = k_{\max}$, giving the most sensitive decay behavior. Let us now consider alternative applications of the method. For example, it is also of interest to detect small effects on nonclassical quantum states in other applications, such as light transmission through media that lead to some decoherence. This is of great importance for applications in quantum communication, where the transmission can be performed via optical fibers or through the atmosphere.

The preparation of photon number states, at least for larger photon numbers, is much more difficult to realize as the Fock-state preparation in the ion trap. However, squeezed light can be used as the nonclassical radiation source for the measurement principle under consideration. For simplicity we will consider a squeezed vacuum. The action of the medium is modeled as before: it acts like energy relaxation in a thermal reservoir. The method, however, is useful also for other sources of decoherence.

Let us consider a squeezed vacuum state, $|\text{sv}\rangle = \exp[-(r/2)\hat{a}^{\dagger 2} + (r/2)\hat{a}^2]|0\rangle$, with $r \geq 0$. In contact with a thermal reservoir, the minimum of the scaled quadrature variance (for $\varphi = 0$ in Eq. (3)) behaves like

$$\langle(\Delta\hat{x}(t))^2\rangle_{\min} = (1 + 2\bar{n})(1 - e^{-2\gamma t}) + e^{-2r}e^{-2\gamma t}, \quad (13)$$

the quadrature being scaled such that the variance in the vacuum state is unity. For the chosen phase $\varphi = 0$ the nonclassical effect is most pronounced. The characteristic function for this phase is simply given by

$$G_{\text{sv}}(k, t) = e^{-k^2\langle(\Delta\hat{x}(t))^2\rangle_{\min}/2}. \quad (14)$$

Its time derivative yields the k -value with the maximum sensitivity of our method to be

$$k_{\max} = \sqrt{2e^{2r}}, \quad (15)$$

which is independent of the value of \bar{n} .

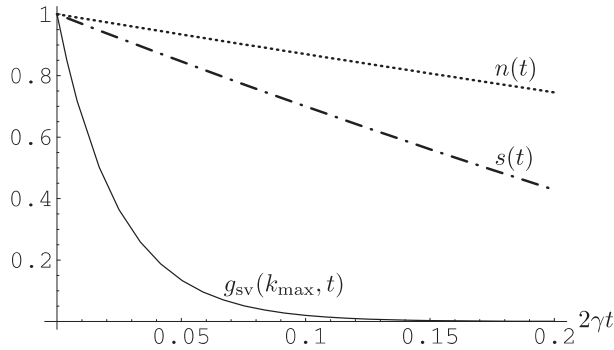


FIG. 3: Time evolution of the normalized mean photon number $n(t)$, the quadrature variance $s(t)$, and the characteristic function $g_{\text{sv}}(k_{\max}, t)$ of an initial squeezed vacuum state with $r = 1.32$, for $\bar{n} = 1$.

In Fig. 3 we show the time evolution of the normalized mean photon number $n(t)$, the normally-ordered quadrature variance $s(t)$, and the characteristic function $g_{\text{sv}}(k, t)$, where $s(t) = \langle :(\Delta\hat{x}(t))^2: \rangle_{\min} / \langle :(\Delta\hat{x}(0))^2: \rangle_{\min}$ and $g_{\text{sv}}(k, t) = G_{\text{sv}}(k, t) / G_{\text{sv}}(k, 0)$. As expected, the fastest decay is observed for the characteristic function at $k = k_{\max}$. To detect this fast behavior, the characteristic function can be derived from the quadrature distribution, for the feasibility of such measurements see [13]. For our method the Fourier transform is needed only for the value k_{\max} and for the phase with the minimal quadrature variance.

In conclusion, we have shown that highly sensitive measurements can be performed by detecting the strongly nonclassical part of the quadrature characteristic function. The method makes use of the high fragility of the nonclassical effects. For example, the direct observation of the characteristic function can monitor the

redistribution of the motional-state occupations of an initially prepared Fock state of a trapped ion. Sensitive optical decoherence measurements can be realized by using squeezed light. The method, which may be useful for highly sensitive noise control in quantum information systems, requires only a unique measurement principle, independent of the used nonclassical state.

-
- [1] H.J. Kimble, M. Dagenais and L. Mandel, *Phys. Rev. Lett.* **39**, 691 (1977).
 - [2] R. Short and L. Mandel, *Phys. Rev. Lett.* **51**, 384 (1983).
 - [3] R.E. Slusher, L.W. Hollberg, B. Yurke, J.C. Mertz, and J.F. Valley, *Phys. Rev. Lett.* **55**, 2409 (1985).
 - [4] C.M. Caves, *Phys. Rev. D* **23**, 1693 (1981); R. Loudon, *Phys. Rev. Lett.* **47**, 815 (1981).
 - [5] M. Xiao, L.-A. Wu, and H.J. Kimble, *Phys. Rev. Lett.* **59**, 278 (1987).
 - [6] P. Grangier, R.E. Slusher, B. Yurke, and A. La Porta, *Phys. Rev. Lett.* **59**, 2153 (1987).
 - [7] E.S. Polzik, J. Carri, and H.J. Kimble, *Phys. Rev. Lett.* **68**, 3020 (1992).
 - [8] U.M. Titulaer and R.J. Glauber, *Phys. Rev.* **140**, B 676 (1965); L. Mandel, *Phys. Scr.* **T12**, 34 (1986).
 - [9] Th. Richter and W. Vogel, *Phys. Rev. Lett.* **89**, 283601 (2002).
 - [10] W. Vogel, *Phys. Rev. Lett.* **84**, 1849 (2000).
 - [11] W. Vogel and D.-G. Welsch, *Quantum Optics* (Wiley-VCH, Weinheim, 2006).
 - [12] W.H. Zurek, *Nature* **412**, 712 (2001).
 - [13] A.I. Lvovsky and J. H. Shapiro, *Phys. Rev. A* **65**, 033830 (2002).
 - [14] S. Wallentowitz and W. Vogel *Phys. Rev. Lett.* **75**, 2932 (1995); *Phys. Rev. A* **54**, 3322 (1996).
 - [15] P.C. Haljan, K.-A. Brickman, L. Deslauriers, P.J. Lee, and C. Monroe, *Phys. Rev. Lett.* **94**, 153602 (2005).
 - [16] D.M. Meekhof, C. Monroe, B.E. King, W.M. Itano, and D.J. Wineland, *Phys. Rev. Lett.* **76**, 1796 (1996).
 - [17] C. Di Fidio and W. Vogel, *Phys. Rev. A* **62**, 031802(R) (2000).
 - [18] P. Marian and T.A. Marian, *J. Phys. A* **33**, 3595 (2000).